FOI

Quantum Radar

The follow-up story

TOMMY HULT, PER JONSSON, MAGNUS HÖIJER

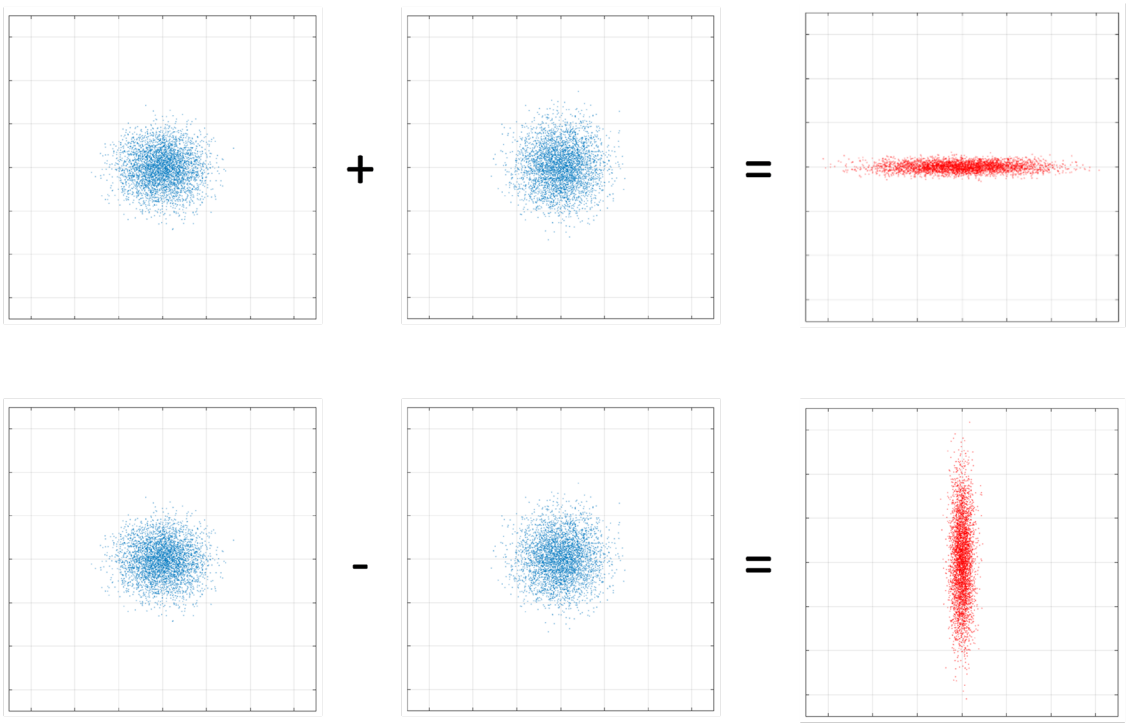

FOI-R--5014--SE
ISSN 1650-1942 October 2020

Tommy Hult, Per Jonsson, Magnus Höijer

Quantum Radar

The follow-up story

Title	Quantum Radar
Titel	Kvantradar - Uppföljningen
Rapportnr/Report no	FOI-R--5014--SE
Månad/Month	Okt/Oct
Utgivningsår/Year	2020
Antal sidor/Pages	45
Kund/Customer	Försvarsdepartementet/Ministry of Defence
Forskningsområde	Telekrig
FoT-område	Inget FoT-område
Projektnr/Project no	A74017
Godkänd av/Approved by	Christian Jönsson
Ansvarig avdelning	Ledningssystem
Exportkontroll	The content has been reviewed and does not contain information which is subject to Swedish export control.

Summary

In the year 2019, a boom is seen for the Quantum Radar. Theoretical thoughts are taken into experimental results claiming a supremacy for the Quantum Radar compared to its classical counterpart.

In 2020, a race between the classical radar and the Quantum Radar continues. The 2019 experimental results are not explicitly doubted. However, it is questioned if the experiments are organised taking the classical radar technology potential fully into account. It is argued, the classical radar, within the technology level of today, should be able to reach the same detection performance as its quantum counterpart.

Simultaneously, the gedanken experiments fully taking the classical radars potential into account, implicitly reveals potential advantages of the Quantum Radar; to work as low-probability-of-intercept (LPI) radar and to retain performance in a heavily contested electromagnetically environment.

Sammanfattning

År 2019 får kvantradarn ett uppsving. Teoretiska tankegångar blir till experimentella resultat visande på kvantradarns fördelar jämfört med dess klassiska motsvarighet.

År 2020 kommer argument på bordet som talar för en klassisk radar. Experimenten som visar på kvantradarns fördelar ifrågasätts inte, men argument framförs att experimenten inte är så utförda att den klassiska radarns fulla potentiella möjligheter utnyttjas. Den klassiska radarn skulle, i alla fall med dagens teknologi, kunna nå samma måldetektionsförmåga som dess kvantmotsvarighet.

Samtidigt och implicit, yppar dessa tankeexperiment kvantradarfördelar; Kvantradarn kan fungera som smygradar (LPI-radar) samt behålla operabilitet i en elektromagnetisk omstridd miljö.

Contents

1 Introduction

In Sweden, the European Union and the rest of the world, substantial efforts are now done with the purpose of realising properties arising from the use of (the second generation) quantum physics. Technology has reached the readiness of going from basic science into actual prototypes.

In 2019 the company Google presented a quantum computer [1] getting an enormous amount of press all around the world. Examples of efforts are, in Sweden the 12 year SEK 1 billion Wallenberg Centre for Quantum Technology (WACT) [2] and in the EU, the 10 year EUR 1 billion Quantum Technologies Flagship program [3].

The largest efforts are put into areas like quantum computing and quantum simulation, but also quantum communication (quantum cryptography, quantum internet) and quantum sensing.

A quantum radar is an example of a quantum sensor with the potential of improving sensor system performances. Its applications is initially assumed mostly military and scientific, potentially there is also medical applications.

The main applications being suggested for a quantum radar as seen of today includes,

- To intercept previously undetected targets
- To gain further knowledge of the targets
- To operate with less risk of being detected
- To operate with less risk of interference
- Improved ability to operate in a heavily electronically contested environment

The first point suggest that objects not intercepted by a classical radar can be intercepted by a quantum radar. A PhD thesis [4] and a book [5] showing the very interesting results of a different radar cross section pattern in the quantum case has been questioned. In 2020 the doubts were further augmented as the authors of [4] and [5] themselves put doubts on their results [6]. The radar cross section is still possibly different in the quantum case due to the material properties of the target being sensed differently in the quantum case, and the second point may be achievable.

The third and fourth point make it possible to operate closer to the target without being intercepted or interfering with others. Consequently, the detection probability of the target is increased.

The last point makes it possible for a quantum radar to act further into an electromagnetically contested environment still being operational.

The scientific interest has been substantially more focused on the field of quantum information processing than the field of detection (e.g. radar), probably due to the larger and more non-military impact of quantum computing, quantum simulation and quantum communication. Similarities between the fields make it possible to harvest from the science developed in the field of quantum information processing, and some thereof presented in this report. Conversely, by studying and potentially unfolding the Quantum Radar, we are simultaneously given insight into the global race of developing and harvesting quantum technology.

Our 2019 report [7], focused on understanding, evaluation and to some degree implications of using quantum physics in radar systems. The intended readership of the report was external and internal. This year's report is written with an intended internal readership, and focusing on understanding and on key technologies.

In chapter 2, we cover the major developments in the field since last year. In chapter 3, we describe and compare major methods to quantify the advantage of one radar system to

another. In chapter 4, we enlighten the difference between discrete and continuous variables in the quantum case, which was a shortcoming in the 2019 report. In chapter 5, we examine possible amplifiers. The possibility to generate sufficiently strong signals to get a practical radar system seems to be a challenge of today. In chapter 6 we review a few experimental realisations of a quantum radar. Our major conclusions are given in the last chapter. In the appendix, we explain the concept of coherent states and some common detection methods.

2 The quantum illumination story revisited

One of the pioneers of quantum radar, Jeffrey Shapiro, has lately presented his view on Quantum Illumination (QI) in a series of paper [8-10]. Shapiro's three papers have the same structure but become more and more detailed for each new version. The latest paper [10] includes more physics and equations to motivate his viewpoints. Most of the history and conclusions in his papers were presented in our previous report [7]. However, some of the findings in his paper can be stressed once more and he gives some comments on the latest all-microwave quantum radar systems [11, 12] that have not been published before.

The general message from Shapiro is that it is difficult to gain an advantage with quantum illumination in realistic radar or lidar applications. It is difficult to achieve quantum receivers that outmatch the results from optimal and existing classical detections schemes. He see more possibilities of using quantum illumination in quantum communication and quantum key distribution [13-18].

In our review of Shapiro's papers, we start with some important points on the receiver difficulties of utilizing quantum illumination. Right after the original proposal by Lloyd using entangled single-photon states [19], Shapiro co-authored two papers. One of the papers showed that the original scheme will not be better than a classical coherent-state[1] radar [20]. The second paper by Tan *et al.* showed that it is possible to gain better performance than any classical system when starting with squeezed states from e.g. spontaneous parametric down-conversion [21]. It is possible to improve the error-probability exponent[2] by a factor of 4 (6 dB) with quantum illumination compared to a classical coherent state, but only in a lossy, noisy and low-brightness signal scenario. These first papers did not give any receiver realization that could use this advantage. None of the standard receivers, based on direct, homodyne or heterodyne detection[3], could provide any advantage because the signature of the state proposed by Tan *et al.* [21] has a phase-sensitive cross correlation, as showed by Shapiro [10].

Guha and Erkmen proposed two receiver realizations that could partly utilize the quantum illumination advantage based on the optical parametric amplifier (OPA) or the phase-conjugated (PC) receiver [22], but at best they could achieve a factor of 2 (3dB) improvement compare to classical schemes, i.e. half of what is theoretical possible. The receivers are possible to realize with today's technology, but they are quite complex and susceptible to experimental nonidealities. For example, the experimental realization of quantum illumination that used the OPA receiver [23] only achieved a 20% (0.8 dB) error probability exponent advantage over a coherent state system although the set-up was idealized and simplified compared to a real lidar system.

There are receiver schemes that in theory could exploit the full advantage. One requires a Schur transform on a quantum computer [24] and the other requires single-photon sensitive sum-frequency generation [25]. Since both of them still are beyond the reach of available technology these methods are mainly theoretical tools for the time being.

[1] Coherent state is explained in the Appendix.

[2] The meaning of error-probability exponent measure can be found in Sec. 3.2.

[3] The different standard detection methods are described in the Appendix.

All of the above receivers require that the reflected signal interfere with the stored idler in the receiver. Shapiro formulates the concept as: “QI can only interrogate a single polarization-azimuth-elevation-range-Doppler resolution bin at a time if it derive its full performance advantage over a conventional radar” [10]. This is quite different to a conventional radar were all ranges can in principle be tested at once. Therefore, it is difficult to take advantage of the full quantum illumination gain when the position of the target is unknown. All ranges must be individually tested and furthermore, the target’s effects on polarization and frequency must be taken into account. An additional complication is that the best current idler storage technique, an optical-fibre delay line, has losses that only allow the quantum advantage to survive for ranges below 11 km [10, 26].

During 2020, other approaches were published where they measured the signal and idler individually and performed the correlation digitally afterwards [11, 12]. This would allow for measuring multiple ranges simultaneously. These schemes should be compared to noise radars rather than a standard radar. The quantum noise radars show a detection improvement compared to their classical noise versions. Since the publications are quite new, preprints of these work occurred in 2019[4], the evaluation of them have just begun. Shapiro is one of the few that has critically analysed the systems [10]. He calls them quantum-correlated noise (QCN) respectively classically correlated-noise (CCN) radar. Shapiro states that the authors have not compared their quantum systems with the optimal classical version. In the classical case, it is possible to use a high-brightness classical noise source and using an asymmetric splitting ratio so that the signal is as weak as the quantum signal while keeping a high-brightness idler. In the quantum source the signal and the idler brightness is always equal. Therefore, the heterodyne detection of the quantum system introduce relative more noise in the receiver than the classical system with a high brightness idler. As a result, the gain from the quantum correlations is cancelled by the higher relative receiver noise. This matter is further discussed in Chapter 6.

As seen from the above summary, Shapiro does not see much use of quantum illumination for practical lidar or radar systems. However, in his exposition he is only comparing the quantum radar with the *optimal* classical radar in terms of detection capability. This is not relevant in all cases. Other considerations may preclude the use of the optimal classical radar. It is however, safe to say that quantum illumination will not outcompete classical radar generally.

Besides the discussion on detection capability, Shapiro treats the choice of wavelength for quantum illumination. Firstly, the technology for quantum system is more mature in the optical region compared to the microwave region. To achieve quantum illumination, the time-bandwidth product should be as large possible. The advantage of quantum illumination, compared to conventional lidar or radar degrades, at constant pulse duration and bandwidth, with increasing signal energy. To maintain the advantage, the time-bandwidth product must increase with the increasing signal energy. The potential maximum time-bandwidth product is higher in the optical regime than in the microwave regime due to the four to five orders higher carrier frequency. On the other hand, quantum illumination only has an advantage over classical counterpart in the region of high loss, low signal brightness and high background. The high background is not normally the case in the optical regime but always the case for microwaves. Barzanjeh *et al.* presented an electro-opto-mechanical (EOM) converter to reach the microwave regime from a source in the optical regime [26], which arouse a large interest. This converter is however intrinsically narrow band so it will be difficult to reach the necessary time-bandwidth product. The Josephson parametric amplifiers (JPA) used in the all microwave

[4] See https://arxiv.org/abs/1903.00101 and https://arxiv.org/abs/1908.03058.

experiments [11, 12] have a higher time-bandwidth product. The maximum dynamical bandwidth of the JPA today, is a few MHz.

A final remark of Shapiro's papers is that he points out that the receiver operating characteristics (ROC) is a far better measure than the normally used error probability, which is further discussed in Chapter 3.

2.1 Microwave Quantum Radar Cross Section

According to several authors [4, 27-29], there were a quantum gain obtained in the targets radar cross section when using a single or a few photons as a radar signal. Through simulations of various geometries it has been surmised that there probably do not exist an extra gain in the sidelobes of the QRCS [30]. This discrepancy is thought being caused by the assumption that the number of incident photon modes on the target has been diminished to one mode only. This would then give the wrong answer since the incident photon should be modelled as a continuous probability function. But in doing so the authors [30] make a new assumption that the probability wave function ψ of the photon behaves as if it is an electric field.

This assumption may or may not be correct, which leads to the conclusion that more research is needed before it is possible to state if there is a gain in RCS or not when using a single or a few photons.

3 Quantification of Quantum Radar Supremacy

3.1 Quantum Supremacy Number

In the literature, there are efforts performed with the purpose of comparing the quantum illumination radar to classical radars. There is, not too uncommon, a will to condense the difference into one number. In the literature, the number 4, or equivalently 6 dB, is mentioned as a possible quantum radar supremacy over a classical radar. The origin of the number 6 dB is an article in Physical Review Letters by Tan *et al*. [21][5]. The number also forms the basis in an attempt to give a system perspective of a quantum radar [31].

The relevant question is what does a number of quantum supremacy mean. In [21], it is described as, "… the quantum-illumination system realizes a 6 dB advantage in the error-probability exponent over the optimum reception coherent-state system." That give us at least three new questions.

1. What is the "error-probability exponent"?
2. Is the "error-probability exponent" the most relevant metric?
3. Why is the comparison done relative to "the optimum reception coherent-state system"?

To address these questions, we need to understand a bit of communication and detection theory. Knowledge thereof also give us abilities to understand the different supremacies claimed in the literature. Our understanding thereof is given in this chapter.

3.2 Error probability bounds

A radar typically has to make a decision whether a target is present or absent. One measure[6] of a radars performance, is to calculate its probability to make a false judgement[7],

$$\mathrm{P}\left(e\right) = P_{ND}\mathrm{P}(H_1) + P_{FA}\mathrm{P}(H_0) = P_{ND}\mathrm{P}(H_1) + P_{FA}\left(1-\mathrm{P}(H_1)\right), \tag{1}$$

where $\Pi(H_x)$ denotes the probability of hypothesis H_x being true. The hypothesis are,

[5] It is a good article giving some of the limits of the quantum radar possibilities.

[6] The measure presented in this section, is common in the literature and relatively easy to use, though it is more designated to be used by the communication community and not so often used by the radar community. This topic is further discussed in section 3.3.

[7] The bold Π denotes probability, and $\Pi(e)$ denotes the probability of making an error e.

$$H_0: \text{ Target absent }, \tag{2}$$

$$H_1: \text{ Target present }, \tag{3}$$

The two remaining quantities in (1) are,

$$P_{ND}: \text{ Probability of not detecting a present target }, \tag{4}$$

$$P_{FA}: \text{ Probability of detecting an absent target (False alarm) }. \tag{5}$$

To find analytic expressions for P_{ND} and P_{FA} are in the classical [32], as well as in the quantum case [21], often daunting tasks. Fortunately, there are expressions giving bounds of the error probabilities. Below we shortly describe two of them, Chernov and Bhattacharyya bounds.

3.2.1 Chernov bound

The Chernov bounds give an upper limit of the probability of a random variable being outside a specific interval around the expectation value of the same random variable. Specific limits are given for both sides of the interval. Chernov bounds can be calculated both in the classical case [32] and in the quantum case [33]. Hence, upper limits can be calculated for both P_{ND} and P_{FA} in (1).

If,

$$\mathrm{P}(H_1) = \mathrm{P}(H_0) = \frac{1}{2}, \tag{6}$$

is assumed, and the discrimination level between the hypothesis H_0 and H_1 in (1) is chosen to minimize the total error probability ($\Pi(e)$), an upper limit for the total error probability can be calculated as well.

Due to the inherent construction of the Chernov bounds [32, 33], the upper limit of the total error probabilities will (when also the above assumptions are included) be of an exponential form,

$$\mathrm{P}(e) \leq \mathrm{e}^{-\alpha\gamma}, \tag{7}$$

where γ is the signal to noise ratio, and α is factor dependent on the technology at use. The question at point 1 in section 3.1 can now be answered; the “error-probability exponent” is the product αγ.

The in section 3.1 also mentioned, “6 dB advantage in the error-probability exponent” implies an increase of α by 6 dB, corresponding to a decrease in total error probability by

17 dB[8]. Equally, it could be described as a processing gain of 6 dB making it possible to detect 6 dB weaker signals.

3.2.2 Bhattacharyya bound

Bhattacharyya bounds are weaker than Chernov bounds. The advantage of Bhattacharyya bounds is that not only upper bounds for the error probability is provided but also lower bounds. The upper Bhattacharyya bound is looser than the upper Chernov bound but may coincide [21]. The lower Bhattacharyya bound is always loose [10]. Examples on Bhattacharyya bounds is given in [21], where the upper bound on error probability for a quantum illumination radar is shown to be below the lower Bhattacharyya bound for a coherent state radar[9].

3.3 Measure of performance

3.3.1 Receiver Operating Characteristics

The second question in section 3.1: is the "error-probability exponent" the most relevant metric? From a radar community perspective, the short answer is a clear no. Firstly, the assumption in (6) of the two hypothesis being equally probable is good in a communication scenario. In a radar scenario, it is not reasonably good; there are often not even good estimates of the probabilities of the two outcomes at hand.

Secondly, a radar engineer does also typically not find the threshold level between the two hypothesis in (2) and (3) by minimising the error probability according to (1). Instead, the trade-off between a low probability of false alarm (P_{FA}) and high probability of detection (P_D),

$$P_D = 1 - P_{ND}\,, \tag{8}$$

is recognized, and described by a Receiver Operating Characteristic (ROC) curve, see Figure 1. The false alarm probability is most often prescribed to be low. A typical prescribed value may be as low as 10^{-9} (false alarm rate of one in a billion), or sometimes ever lower.

[8] 10*log10(exp(10^(-6/10))) = -17.3 dB

[9] The coherent state radar is according to the authors, the toughest benchmark.

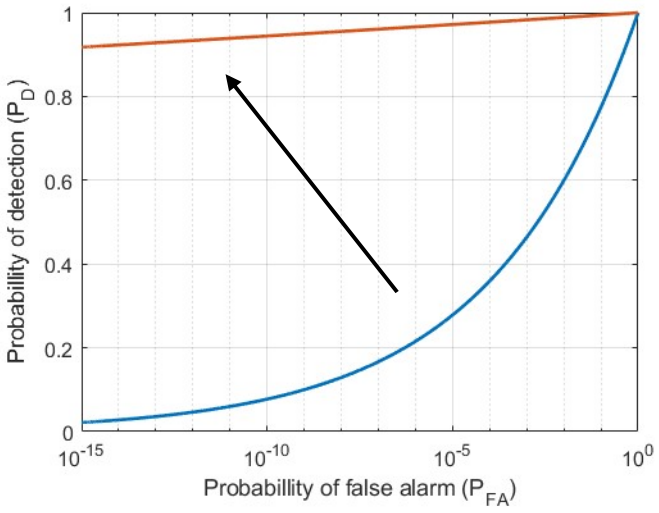

Figure 1: A Receiver Operating Characteristic (ROC) curve shows the trade-off in a detector between the acceptance level of false alarm (P_{FA}) and the probability of detection of a present target (P_D). The blue ROC-curve can be pushed toward the red ROC-curve, by accepting decreases in radar performances like shorter range and longer reaction time. Alternatively, the improvement can be reached by new detection algorithms and technologies, whereof the quantum radar is one opportunity.

With a prescribed false alarm probability, the detection probability is in principal given by the ROC. However, there are techniques to push the ROC curve toward the upper left corner. One is to get a higher signal to noise ratio, typically corresponding to a shorter range of the radar. Another to increase the bandwidth[10] and/or increase the (coherent) integration time, corresponding to a longer reaction time of the radar. Still another possibility is to introduce new methods and technologies, whereof the quantum radar is one opportunity.

3.3.2 Performance metric in use

The supremacy of using ROC as a performance metric is fully recognized by Shapiro, "… ROC is crucial because it is a far better target-detection performance metric than error probability, as radar targets should not be presumed equally likely to be absent or present." [9, 10]. It is somewhat surprising that a substantial part of Shapiro's article [10] focus on error probability and the error-probability exponent. Two reasons therefore, Shapiro in [10] reviews important work by other authors[11]. Secondly, the ROC curve describe the detection performance exhaustively, but it may be hard to quantify the advantage of one ROC curve to another.

An attempt to quantify the difference of two experimental ROC curves is done by Luong *et al.* [11, 34]. They compare their quantum radar with a classical radar having as similar properties (including integration time) as possible. The quantum ROC curve shows substantially better properties than the classical one, see Fig. 10 and 12 in [11]. By

[10] Practical limitations may limit the use of a larger bandwidth.

[11] A closer look upon the articles quoted by Shapiro will however in many cases reveals Jeffrey Shapiro as a co-author.

reducing the integration time of the quantum radar by a factor of eight, while keeping the integration time of the classical radar constant, the ROC curves of the quantum radar and the classical radar show similar performances, see Fig. 12 in [11]. Hence, one could say that in the specific experiment in [11], the quantum radar shows an experimental factor of 8 or 9 dB supremacy over the correspondent classical radar.

However, the comparison method applied by Luong *et al*. assumes the form of the ROC curve being the same in the two cases. The ROC curve data in [11] is somewhat limited[12] and it is not completely clear the assumption being fulfilled.

Finally, even it is not possible to condense the comparison between different technologies into one number; the comparison of ROC curves will provide the radar engineer with a tool to evaluate different radar technologies.

[12] The limited amount of data is not surprising. To perform measurements of small probabilities are time consuming.

4 Discrete and Continuous Variables

In our 2019 report [7], we describe the key physical concepts, Quantum Superposition and Entanglement. These concepts are fundamental physical properties and essential for understanding the Quantum Radar experiments described in the latter part of the 2019 report.

However, there is a missing point not addressed. Quantum superposition is presented using polarization as an example. Polarization has two degrees of freedom, exemplified by vertical ($|V\rangle$) and horizontal polarization ($|H\rangle$). In contrast, in the described experiments, the in-phase and quadrature components of the field are used. They may take any value and span an infinite dimensional space.

In this chapter, we put light onto this discrepancy, and address why the continuous field components rather than the discrete polarization have been used in the articles described in [7]. Essential references to this presentation are [35-39]. Substantial lists of further references are given in [35-37]. The focus of [35-39] is Quantum Information Processing (QIP) reflecting its general larger technological impact relative to Quantum Radar. However, much of the physics is the same, and the description can be reused.

4.1 Introduction to Discrete and Continuous Variables

Field values, like the electric and magnetic field, have a continuous degree of freedom. At the same time, the electromagnetic interaction may be described by photons, who have a discrete degree of freedom (1, 2, 3 …). It is somewhat similar to the classical difference between an analog and digital description (technology).

Quantum mechanics is assumed giving a complete description of physics[13]. Most quantum systems have both discrete and continuous degrees of freedom. A complete description of the electromagnetic field are to take into account all degrees of freedom, i.e. photon number, wavelength, polarization and wave vector [38].

If the variable we choose to encode and observe is discrete (having discretized eigenvalues), we have a discrete variable (DV) technology. Similarly, if the variable we choose to encode and observe have a continuum of eigenvalues, we have a continuous variable (CV) technology.

Ultimately, the choice of measurement decides if we have a discrete variable or continuous variable. As an example [38], take a single-photon state, it is obviously discrete, but we may choose to measure quadrature components of the electromagnetic field which are continuous variables. However, in most, not to say all, practical technologies it is preferable to generate and measure the same kind of variable (CV or DV). The polarization has always a binary degree of freedom[14].

Simultaneous use of discrete and continuous variables is at the focus of both theoretical and experimental research [39], but outside the scope of this report.

[13] Gravity is an exception, where a good quantum physics model is missing.

[14] The polarization binary degree of freedom is probably a reason why it is often used both as a standard example in textbooks as well as in practical applications.

4.2 Measurement of discrete and continuous variables

In section 4.1, we saw that a single photon could be information carrier of both discrete and continuous variables. Detection of discrete variables (DV) are inherently connected to the use of photon counting detectors. Continuous variables (CV) may be detected using homodyne detection, where the signal is multiplied with a (strong) local oscillator.

In principal, there is no correlation between the choice of CV or DV and the choice of numbers of photons (signal strength) in the set-up. From a measurement perspective, the opposite is true; at least today. Photon detectors works well for a small number of photons but for large photon number states, they fail to measure the photon state [38]. On the other hand, measuring quadrature components of the field, can preferably be done with strong signals and standard measurement equipment may be used [11]. The challenge is to generate strong signals being entangled [7], or signals at least possessing a remaining correlation at the detector larger than what is classically achievable [21].

4.3 Conditionalness and uncertainty

We now look upon pros and cons of continuous and discrete variables from a more theoretical viewpoint [35]. A typical discrete variable case is a single photon carrying information in its polarization. The polarization information can be reliably received in the detector. However, the detection is conditional. The generation of single photons is random in time. The same goes for lost photons in the transmission from generator to detector. Detection can be performed “once in a while” [19].

Contrary, continuous variables can be *unconditional*. E.g. entangled states of field quadrature components can be generated every inverse bandwidth time [35]. However, the unconditionalness comes with a price, *uncertainty*, prescribed by the Heisenberg uncertainty relation. There is always a quantum uncertainty associated with e.g. the quadrature components of the electromagnetic field.

The uncertainty in one of the quadrature components can however be decreased at the expense of a higher uncertainty in the orthogonal quadrature component. The phenomenon is called squeezing and we will look into it in the section 4.4.

In Table 1, we have summarized pros and cons of discrete variables (DV) and continuous variables (CV). In addition, discrete variables in practice imply low signal levels but continuous variables imply higher signal levels. As of today, continuous variables seem to be the most promising technology, and it has been used in reported experiments [11, 12].

Table 1: Pros and cons of using discrete variables (DV) and continuous variables (CV).

	DV	CV
Pros	No uncertainty	Unconditional
Cons	Conditional on rare events	Heisenberg uncertainty

4.4 Squeezing

4.4.1 Squeezed vacuum state

As described in section 4.3, continuous variables come with an inherent uncertainty. Even the vacuum state ($|0\rangle$), having zero photons, has an uncertainty. The left part of Figure 2 shows samples of the quadrature components (i and q) of the vacuum state field. Every little blue dot corresponds to one sample of a field measurement. In total, there are 4000 samples in the figure. The quadrature components are Heisenberg minimum uncertainty states fulfilling[15],

$$\Delta i_0 \Delta q_0 = 1\,, \tag{9}$$

where Δi_0 and Δq_0 are the vacuum state standard deviations of i and q, respectively.

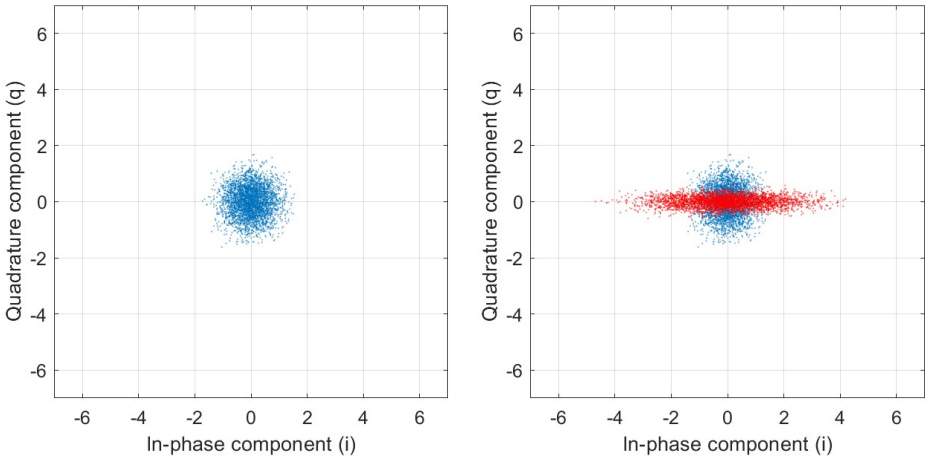

Figure 2: The left figure show 4000 samples from a Heisenberg minimum uncertainty vacuum state. In the right figure, 4000 samples (in red) of a squeezed Heisenberg minimum uncertainty vacuum state has been added.

The left part of Figure 2 shows the uncertainty being equally distributed on both quadrature components.

$$\Delta i_0 = \Delta q_0 = 1\,. \tag{10}$$

However, the uncertainty does not need to be equally distributed on the two quadrature components. In squeezing, the uncertainty is increased in one quadrature component and decreased in the other. In the right part of Figure 2, the red dots are samples from a

[15] The quadrature components have been normalized making the minimum uncertainty product equal to 1.

squeezed vacuum state ($|s\rangle$). The blue dots is the original vacuum state of the left figure. The squeezed vacuum state is still a minimum uncertainty state fulfilling,

$$\Delta i_s \Delta q_s = 1 . \tag{11}$$

However, the standard deviations of the two quadrature components are now different,

$$\Delta i_s = \mathrm{e}^{r} \Delta i_0 , \tag{12}$$

$$\Delta q_s = \mathrm{e}^{-r} \Delta i_0 , \tag{13}$$

where r is called the squeezing parameter [35]. The squeezed vacuum state, in contrast to the vacuum state, does not have zero photons, but instead the expectation value is $\sinh^2 r$.

4.4.2 Two mode squeezed vacuum (TMSV) state

In the reported experiments by Luong et al [11] and Barzanjeh et al [12], the two mode squeezed state generated by the Josephson Parametric Amplifier (JPA) is the epicentre of the technology. In the JPA the two signals, called signal and idler, are generated. In similarity to Figure 2, we have in Figure 3 plotted quadrature values of 4000 samples of both the signal (left) and idler (right). They both look very similar to the vacuum state in Figure 2, both with a Gaussian distribution of both quadrature components. However, they are thermal states, with a larger standard deviation, which can be noticed in Figure 3 by the larger spread of the samples from the origin, compared to Figure 2. The expected number of signal photons (n_s) and idler photons (n_i) is [35],

$$\mathbf{E}\{n_s\} = \mathbf{E}\{n_i\} = \sinh^2(r) . \tag{14}$$

Again, the squeezing parameter (r) has been introduced indicating that squeezing and entanglement is in some way involved in the generation of the signal and idler in the JPA.

Separately, the signal and idler are in thermal states, but any linear combination of them will reveal they being entangled, and the linear combination being in a squeezed state. In Figure 4, the sum of the signal and idler in Figure 3 is shown in the left part, the difference in the right part. These are squeezed states with standard deviations [35],

$$\Delta(i_s + i_i) = \sqrt{2}\mathrm{e}^{r} , \tag{15}$$

$$\Delta(q_s + q_i) = \sqrt{2}\mathrm{e}^{-r} , \tag{16}$$

$$\Delta(i_s - i_i) = \sqrt{2}\mathrm{e}^{-r} , \tag{17}$$

$$\Delta(q_s - q_i) = \sqrt{2}\mathrm{e}^{r} . \tag{18}$$

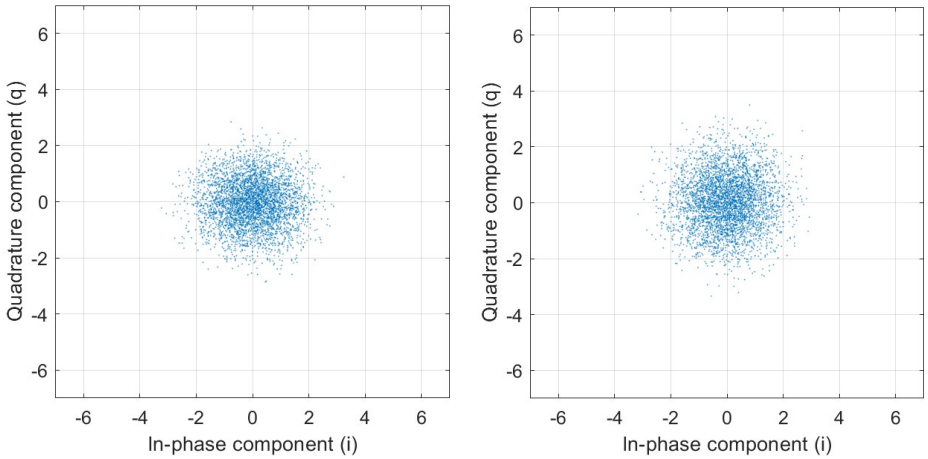

Figure 3: The left (right) figure shows the quadrature components of the signal (idler) generated by the Josephson Parametric Amplifier. They are both in a thermal state.

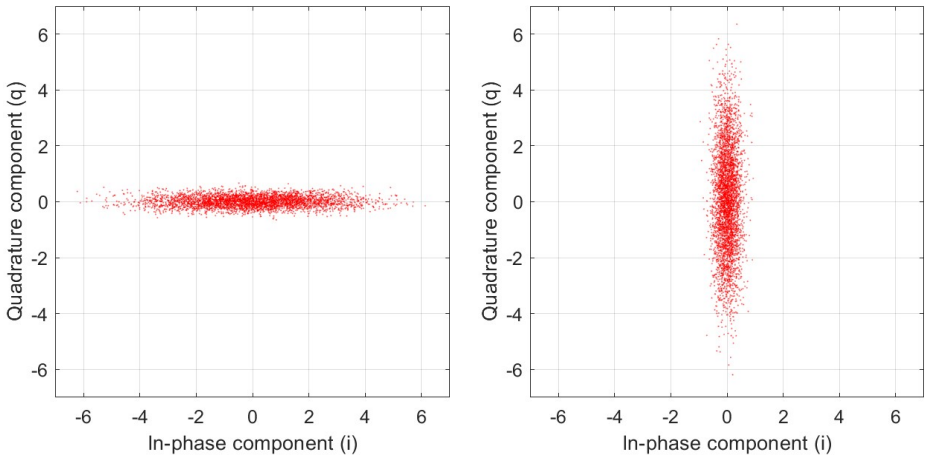

Figure 4: The left (right) figure shows the sum (difference) of the signal and idler in Figure 3. These are squeezed states. The signal and idler are entangled. These states can only be generated by access to both signal and idler.

Anyone having access to only the signal or idler can only measure nothing but the thermal noise in Figure 3, but having access to both the signal and idler makes it possible to measure a much smaller uncertainty according to (16) and (17). Differently stated, a strong correlation can be found between the signal and idler, stronger than any possible classical correlation.

4.4.3 Entanglement for continuous variables and beyond

In section 4.4.2, it was stated that the outcome of a JPA is a signal and idler whose pairs of quadrature components can be strongly correlated. The definition of entanglement for continuous variables is a correlation stronger than what is possible to achieve by any classical state.

However, in practical set-ups in the microwave regime [11, 12], there is a need for noise-adding amplifiers and the environment will add further noise. With the technology of today, the entanglement criterion is broken before reaching the detector [11, 12]. How can a quantum gain compared to the classical benchmark still be reported [11, 12]?

Tan [21] gives one answer. To the classical signal, the same noise will be added as to quantum signal. The entanglement criterion might be broken, but there is still a remaining correlation in the quantum case, stronger than achievable in the classical case.

5 Amplification of entangled states

5.1 Background

With the invention of masers in the 1950's it was possible to amplify signals with much less added noise. This triggered the race to find a lower limit of the added noise in an amplifier, and a lot of interest in the quantum limit, since it now seemed possible to reach.

5.1.1 Noise

For classical electronics, the thermal Johnson noise generated by thermal agitation of charged carriers inside a conducting material is normally modelled as additive white Gaussian noise (AWGN) and its power spectral density as $P_{N_0} = k_B T$ [W/Hz], where k_B is Boltzmann's constant and T is the temperature in Kelvin.

A more general model [40, 41], which include quantum systems can be modelled as the probability that a system (e.g., an amplifier) spontaneously will go from one energy state to another. This is given by the probability density function $(e^{hf/k_B T} - 1)^{-1}$ ("shot noise") and will then result in the power spectral density of the noise [42, 43],

$$P_{N_0}(f,T) = hf \cdot \frac{1}{e^{hf/k_B T} - 1} \xrightarrow{hf/k_B T \ll 1} P_{N_0} \approx k_B T . \tag{19}$$

In the limit of high temperature and low frequency ($k_B T \gg hf$), see Figure 5, P_{N_0} is reduced to Johnson thermal noise which is the optimal classical noise. In the opposite limit, low temperature and high frequency ($k_B T \ll hf$), P_{N_0} is reduced to quantum noise which is the optimal case in quantum systems.

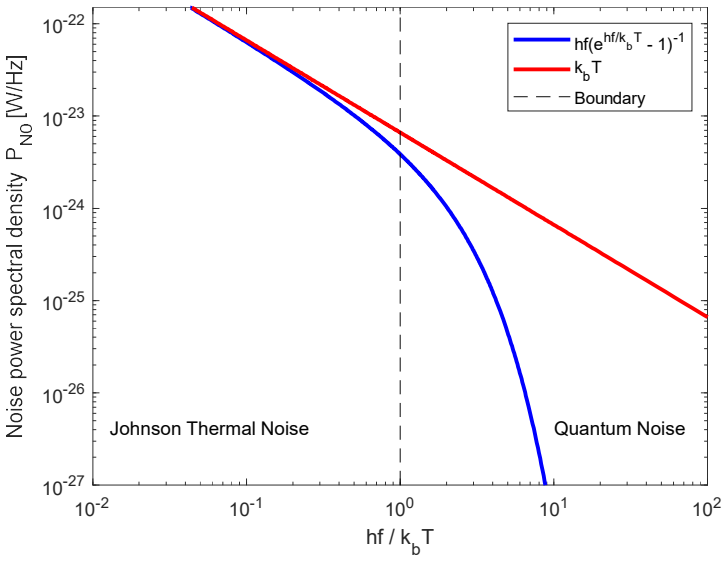

Figure 5. Showing the power distribution and the boundary between Johnson Thermal Noise and Quantum Noise. This boundary is where $k_b T$ is not sufficient to describe the distribution. In this example frequency is fixed at 10 GHz and the temperature is varied between 4.8 mK and 48 K. The boundary is in this example at 0.48 K.

From this follows that if, e.g., we want a quantum amplifier for 1-10 GHz with optimal noise performance the noise-temperature of the amplifier must not be higher than 48 mK.

Further, the bandwidth B of the noise must be much smaller than the carrier-frequency, ($B \ll f$, the narrow band approximation), so that each frequency can be treated as a single complex-valued number.

5.2 Amplifiers

5.2.1 MASER

The *Microwave Amplification by Stimulated Emission of Radiation* is a type of low-temperature (low-noise) amplifier that was invented in the 1950s and is the same principle as a LASER but for microwave frequencies instead of light. Pros: This is a high gain ultra low-noise amplifier with a lower noise level limit of ~1-2 photons per mode at milliKelvin temperatures. Recently [44], a solid state continuous wave maser has been developed that can operate at room-temperature and could potentially give a high gain at ultra low-noise levels of about 4-5 photons per mode. Cons: Very narrow bandwidth, a complex device and needs cooling because of the high-powered supply providing the power of the amplifier.

5.2.2 HEMT

High-Electron-Mobility-Transistor amplifiers is a solid-state transistor that has a possibility of wide-band power amplification. Pros: can amplify up to several 10's of Watts and have extremely high bandwidth. Cons: The lower noise level limit for this type of amplifiers is about 20 photons per mode at milliKelvin temperatures.

5.2.3 Parametric amplifiers

The parametric process works by modulating an energy-storing component like a capacitance or inductance with a harmonic signal. This will result in a mixing process that will transfer energy between the resonant modes of the system. This can be used for amplification of a signal or the creation of entanglement. The device often used for this in quantum technology is the *Josephson Parametric Amplifier*. See [7] for an introduction to the JPA.

There are two types of parametric amplifiers:

- *Phase-preserving amplifiers,* which amplifies with the same gain G no matter what the phase value is.
- *Phase-sensitive amplifiers,* which amplifies with different gain $G = \sqrt{G_I G_Q}$ depending on the phase value, where G_I and G_Q are the quadrature gains.

These amplifiers can operate in either *degenerate* or *non-degenerate* mode of operation:

- *Non-degenerate parametric amplifiers* use different frequencies for the *input*- and *idler*-signals, and its operation was described in [7]. Consequently, the output from the amplifier separates into signal- and idler-frequencies.
- *Degenerate parametric amplifiers* use the same frequency for *signal* and *idler*, so there is only one signal in to the amplifier and one amplified output signal.

Both these modes of operation have a pump-signal on twice the frequency of the mean frequency between *signal* and *idler,* to supply the energy for the amplification.

5.2.3.1 Low-Noise amplification of weak signals using JPA

Assuming the narrowband approximation applies, the input signal is modelled as a narrowband signal and therefore allows us to model it as an analytical signal,

$$\begin{aligned} S^{in} &= (X_I^{in}\cos(\omega t) + N_I^{in}\cos(\omega t)) + (X_Q^{in}\sin(\omega t) + N_Q^{in}\sin(\omega t)) = \\ &= \mathrm{Re}\left\{\left(X_I^{in} + jX_Q^{in}\right)e^{-j\omega t} + \left(N_I^{in} + jN_Q^{in}\right)e^{-j\omega t}\right\} \end{aligned}, \tag{20}$$

where $\left(X_I^{in} + jX_Q^{in}\right)$ is the baseband signal that modulate the carrier signal $e^{-j\omega t}$. The quantities X_I^{in} and X_Q^{in} are the amplitudes of the two quadratures of the signal and $\left(N_I^{in} + jN_Q^{in}\right)$ is a complex-valued noise. The statistical properties of the noise process does not change when multiplied with a complex exponential.

The most common amplifier type is a *degenerate phase-preserving parametric amplifier*, which means that it will amplify both quadratures by the same gain *G* and the output signal is on the same frequency *f* as the input signal (no idler signal),

$$\begin{aligned} &S^{out} = \sqrt{G}\cdot\mathrm{Re}\left\{\left(\left(X_I^{in} + jX_Q^{in}\right) + \left(N_I^{in} + jN_Q^{in}\right)\right)e^{-j\omega t}\right\} \quad \Rightarrow \\ &\Rightarrow \quad X_I^{out} = \sqrt{G}\cdot X_I^{in} + N_I^{out}, \quad X_Q^{out} = \sqrt{G}\cdot X_Q^{in} + N_Q^{out} \end{aligned}. \tag{21}$$

Assuming that we have a narrowband signal the quantum-limit for a *phase-preserving amplifier* can be described by a single number of added noise photons *N* per mode [40], see also (24).

The minimum noise power at the amplifier output can be defined as [45],

$$\min\left(P_N^{out}\right) = (G-1)hfB, \tag{22}$$

and the minimum noise added by the amplifier can then be written as the minimum noise at the output of the amplifier divided by the amplifier gain,

$$\min\left(P_N^{in}\right) = \frac{1}{G}(G-1)hfB. \tag{23}$$

Dividing both sides with *hfB* will give the added minimum number of noise photons per mode in the amplifier,

$$N^{in} \geq \left(1 - \frac{1}{G}\right). \tag{24}$$

The temperature that must be attained to reach this limit can be calculated from,

$$\frac{1}{e^{hf/k_BT} - 1} = \left(1 - \frac{1}{G}\right) \quad \overset{G \neq 1}{\Leftrightarrow} \quad T = \frac{hf}{k_B}\left[\ln\left(\frac{2 - \frac{1}{G}}{1 - \frac{1}{G}}\right)\right]^{-1}, \tag{25}$$

and, e.g. with f =10 GHz and an amplification of G = 3 we need an amplifier temperature of ~0.52 K to get minimum noise. The term $\left(e^{hf/k_BT} - 1\right)^{-1}$ is the radiation density of thermal noise at the temperature T, see section 5.1.1 and [46].

Since the input signal quantum limit is ½ photon (i.e. the Heisenberg limit) then for the case of G = 1, the amplifier adds no extra noise photons to the signal and the output quantum limit will be ½ photon (but to reach this limit it is necessary to cool the amplifier to absolute zero). For gains higher than unity, the added noise is about one photon.

The corresponding quantum limit for a *phase-sensitive parametric amplifier* is when we replace the single gain G with the geometric mean of the quadrature gains G_I and G_Q and get [46],

$$N_I N_Q \geq \frac{1}{4}\left(1 - \left(G_I G_Q\right)^{-1/2}\right)^2. \tag{26}$$

Substituting N_I and N_Q by $N/2$, and G_I and G_Q by G, gives (24). The expression in (26) can be seen as the *phase-sensitive parametric amplifier uncertainty principle*. In this operating mode, it is possible for one of the noise numbers (N_I or N_Q) to be lower than the quantum limit (but it also means that the other noise number must increase with a corresponding amount). This represents a squeezing of the total noise.

5.2.3.2 Generation of Entanglement

As was shown in [7], to generate entangled photons, the JPA is set to work as a *non-degenerate phase-sensitive parametric amplifier.* In a non-degenerate amplifier, the amplified signal is split into two signals on different frequencies. Therefore, the mixing process results in squeezing of the noise difference instead of squeezing the noise itself, as is done in a degenerate amplifier with only one output signal and one output frequency.

The input signal to the amplifier is connected to a cavity that generates a vacuum noise signal, which is amplified by the energy of the *pump*-signal and split into the two different frequencies. This is then called *two-mode squeezing*. If the squeezing result in a noise quadrature-difference that is below the quantum limit, then there is entanglement between the *signal* and *idler* output.

5.2.3.3 Cooling of quantum devices

To achieve the low-noise operations necessary in sections 5.2.3.1 and 5.2.3.2 it is required to reach at least below 50 mK in operating temperature of the amplifier. This is done by cooling the device in several steps, for example,

step 1. cool down to 77K using liquid Nitrogen
step 2. using a liquid Helium (^{4}He) bath to get to 4.2K
step 3. A vacuum pumped (^{4}He) bath to get ~1K
step 4. A (^{3}He) refrigerator to get ~600 mK
step 5. A (^{3}He+^{4}He) mixing bath to reach ~20 mK

This cryogenic dilution freezer is a complicated device that is both expensive and bulky to build, but is commercially available from a few companies.

5.3 Transmitter power of a Quantum radar

Photons have an intrinsic energy of $E=hf$, where h is Planck's constant and f is the frequency. In the radar application there is a compromise concerning frequency that it is necessary to optimize if the radar is to have any practical purpose, see [7]. This approximately result in a frequency in the microwave range of 3 – 10 GHz.

The amplification obtained by the JPA is dependent of the;

- Bandwidth of the JPA cavity (since Q $\approx f_c/BW$, where f_c is the carrier frequency and BW is the bandwidth).
- Power of the pump-signal (since the JPA transfers power from the pump-signal to the amplification process).
- Power-limit of the non-linearity of the JPA (the amplification process only work when the JPA operates in the non-linear region).

The non-linearity is the main limiting factor, so the power output from the JPA will, for a carrier frequency of 10 GHz, be in the range of -201 dBm to -130 dBm (which corresponds to an amplification of 0 – 70 dB) using components at the present level of research. As an example [11] a power of -146 – -141 dBm is attainable from the JPA for the chosen carrier frequency range of 3 to 10 GHz.

5.3.1 Preserving Quantum Correlation in Amplification

The entanglement created in the JPA between photons start to degrade immediately as soon as they leave the JPA, but a lingering extra correlation remains between the photons that can be exploited in the signal processing.

To assess this extra correlation from the quantum entanglement, two radar transmitter systems will be compared. The classical system transmitting a two-mode classical noise signal and a quantum system transmitting a two-mode squeezed vacuum signal (entangled).

The simple set-up can be seen in Figure 6 [47]. For simplicity, both modes in both systems are amplified by the same amount G and the signals of the two systems are processed in the same way.

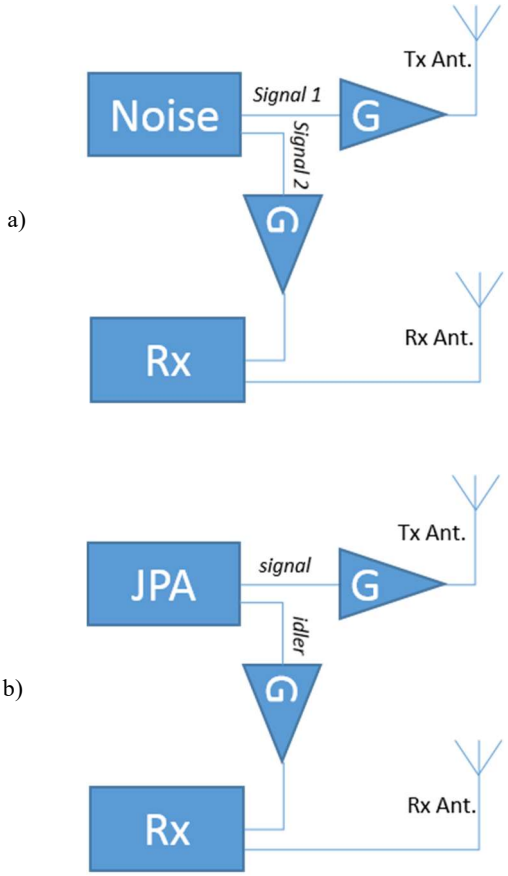

Figure 6. Showing the two radar types, classical type a) where Signal 2 (or 1) is a copy of the generated noise in Signal 1 (or 2) but on different frequencies (modes), and the quantum type b), where two entangled noise signals are created (signal and idler) on two different frequencies (modes). In both cases the signals are amplified with the same gain G.

To compare the input *signal/Signal 1* and *idler/Signal 2* of both amplifier systems a covariance matrix for the radar receiver is set-up for each system that can then be compared.

If input signals to the classical amplifier is (index 1 is the input signal, and index 2 is the idler) $C = \left[X_I^1 \quad X_Q^1 \quad X_I^2 \quad X_Q^2 \right]^T$, the covariance matrix $R_C = E\left\{ CC^H \right\}$ for the classical two-mode noise radar is [47],

$$R_C = \begin{bmatrix} \sigma_1^2 & 0 & \rho_C\sigma_1\sigma_2 & 0 \\ 0 & \sigma_1^2 & 0 & \rho_C\sigma_1\sigma_2 \\ \rho_C\sigma_1\sigma_2 & 0 & \sigma_2^2 & 0 \\ 0 & \rho_C\sigma_1\sigma_2 & 0 & \sigma_2^2 \end{bmatrix}, \tag{27}$$

and $\sigma_1^2 = \sigma_2^2 = (N_s + n_C)/2$, where N_s is the number of signal photons (or signal power if multiplied by hfB) of the source and n_C is the added number of noise photons (or noise power if multiplied by hfB) due to the amplifier. If $\rho_C\sigma_1\sigma_2 = N_s/2$, the correlation can be calculated as [47],

$$\rho_C = \frac{N_S}{N_S + n_C} = \frac{SNR_C}{SNR_C + 1}, \tag{28}$$

where $SNR_C = N_S / n_C$ (the number of signal photons relative to the number of amplifier added noise photons). Figure 7 shows the correlation as function of the input signal power ($N_S \cdot hfB$). The number of noise photons (n_C) is assumed approximately one photon per mode as an example of a JPA. Hence, the noise power is $n_C \cdot hfB \approx hfB$.

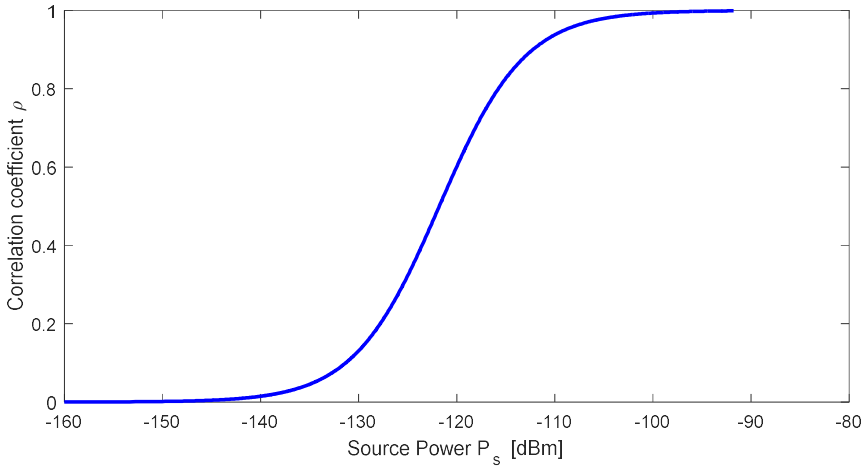

Figure 7. The correlation coefficient dependency on source power (signal power). The noise power is assumed constant at approximately one photon per mode. The frequency is 10 GHz and the bandwidth 100 MHz.

For the quantum system, the covariance matrix R_Q looks almost identical to the classical one, in (27), except for a negative sign that will add an anti-correlation,

$$R_Q = \begin{bmatrix} \sigma_1^2 & 0 & \rho_Q\sigma_1\sigma_2 & 0 \\ 0 & \sigma_1^2 & 0 & -\rho_Q\sigma_1\sigma_2 \\ \rho_Q\sigma_1\sigma_2 & 0 & \sigma_2^2 & 0 \\ 0 & -\rho_Q\sigma_1\sigma_2 & 0 & \sigma_2^2 \end{bmatrix}, \tag{29}$$

The correlation coefficient ρ_Q will therefore be slightly different [47],

$$\rho_Q = \frac{SNR_Q}{SNR_Q + 1} \cdot \sqrt{1 + \frac{1}{N_S}}, \tag{30}$$

for the *two-mode squeezed vacuum* [47]. The enhancement Q_E achieved at the receiver by using quantum entanglement is $Q_E = \rho_Q / \rho_C$, as can be seen in Figure 8. This quantum enhancement does not rely on whether there remain any entanglement in the signal at reception and is related to the quantum information concept of *Quantum Discord* [48].

Since the noise is about ~1 photon in a JPA, the increase of signal power means that the SNR increase. So, from Figure 8b, it can be seen that if amplification of the signal and thereby the increase of SNR is achieved through extra amplifiers, the quantum enhancement will be lost and we only have classical correlation [11, 46-49].

a)

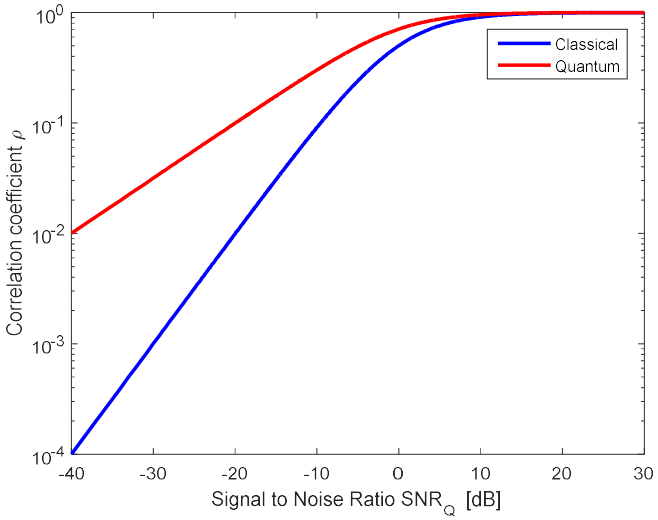

b)

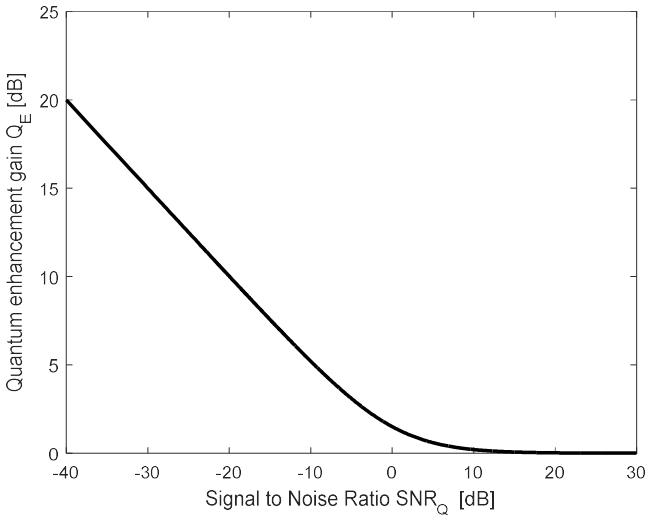

Figure 8. The 'blue' graph in figure a) is the same as the graph in Figure 7, but with a logarithmic axis for the correlation and SNR instead of the signal power on the x-axis. The top figure a) show the dependency between correlation and SNR for classical and quantum systems. The quantum enhancement at the receiver is the ratio between the 'red' and 'blue' graphs in a), and is shown in b).

5.4 Concluding remarks on amplification of an entangled signal

The only amplifier of today that can amplify an entangled signal with very little added noise is the JPA, and even a higher power can be achieved through connecting several JPA together or using a *Josephson Travelling Wave Transmission Parametric Amplifier* (JTWTA) [50]. Theoretically, this will not be enough since when the power of the signals increases, the correlation gain decreases.

This conclusion is based on the assumption that both *signal/Signal 1* and *idler/Signal 2* are amplified with the same gain. This does, however, not seem to be the optimal solution [47]. According to Agarwal et al. [51], for a two-mode squeezing laser amplification the results show that the quantum enhancement is more robust if only the *signal* (or *idler*) is amplified while the *idler* (or *signal*) is not amplified. This might be a way to amplify the quantum radar signal so that it can be used at normal radar target distances.

6 Experimental realizations of quantum radar

The recent experimental results of Luong *et al*. [11] and Barzanjeh *et al*. [12] are interesting for many reasons. They are in the microwave regime were quantum illumination has the highest potential due to the intrinsic high background. They are all microwave set-up, which means that the complex electro-opto-mechanical (EOM) converter [26] is not necessary. The JPA used as entanglement source, which potentially has a broader bandwidth compare to the EOM. The most important advantage is that their scheme allow for separate measurement of the idler and reflected signal and the correlations are tested in the digital regime afterwards. In this way, it is possible to probe all ranges in the post processing stage in contrast to previous quantum illumination schemes where one range can be tested at a time since the reflected signal must be overlapped with idler at the detector.

The two schemes are quite similar. Both groups are using a Josephson Parametric Amplifier (JPA) as a source of entangled two mode squeezing and amplifying both the signal and idler using HEMT amplifiers before leaving the cryostat. The quadrature components (i and q) of the idler is measured directly in a heterodyne detection digitizer while the signal is sent to an antenna. The return signal is collected with a second antenna and the quadrature components measured in another heterodyne detection digitizer. The correlation between the returned signal and idler is investigated digitally. They compare the quantum set-up with a classical set-up where they replace the JPA source with a classical noise source with the same output power as the JPA. Otherwise, the set-up is identical for the two set-up, i.e. the signal and idler are amplified and detected with the same components as before. Both groups saw a detection improvement with the quantum source (JPA) compared to the classical noise source. Barzanjeh *et al*. [12] also compared the two set-ups with coherent-state illumination using both heterodyne and homodyne detection. The results show that both the coherent-state illumination schemes is better than quantum and classical noise radar. However, when calibrated for the noise in the idler arm, the quantum noise radar give similar results as the homodyne detection and outperforms the heterodyne detection. The calibration is not an option in a real radar system, but shows the potential of the quantum noise radar if the idler can be measured without amplification. Anyway, the coherent-state illumination is not a good option in application where you normally use noise radars, since it is easier for an adversary to detect a coherent-state signal compared to a noise signal.

None of the groups compared their results with the scheme suggested by Shapiro [10], where the noise signal is asymmetric divided to a high brightness idler and a weak signal that matches the output of the noise radar. He claims that the quantum noise radar cannot outperform this scheme (see also Chapter 2). It is still unclear for us if Shapiro's argument hold for all possible ways to perform the heterodyne measurement of the idler and we need to investigate it further.

Even though it would be possible to circumvent Shapiro's objection, the experimental systems described above have merits that is far from what is needed in a useful radar for longer ranges. As described in Chapter 5 it is difficult to simply amplify the signals to useful levels and retain the quantum advantage. Asymmetric amplifications of the signal and idler might be a solution [47, 51], especially if the idler could be measured without amplification. A larger time-bandwidth product of the source and the detection system will allow for quantum advantage at higher output power. There are several ways to improve the components in the system. Some suggestions are presented in a recent paper of Luong *et al*. [34].

7 Conclusions and Future Work

To generate entangled continuous variables (in contrast to discrete variables) seems to be the most promising technology due to higher signal levels and unconditional generation and measurements of entangles states.

Error probabilities are often used to quantify the performance of a quantum radar. A plausible reason is the demand for a simple metric of performance. However, error probabilities being a good metric in the quantum case is not a good metric in the radar case. The use of Receiver Operating Characteristic curves is more adequate, but it leaves the radar engineer with a more complex task in comparing a quantum radar to a classical radar.

To utilize the full 6 dB advantage of a quantum radar suggested by Tan *et al*. [21] is not possible with today's technology and not useful for most practical radar application since it can only interrogate one distance at the time. More interesting is the quantum version of a noise radar [11, 12] where it is possible to interrogate all distances similar to a conventional radar. There are however doubts if this scheme can be superior to an optimal designed classical noise radar [10]. This objection needs to be further analysed. Furthermore, there might be other protocols for quantum illumination that could avoid the objection [52].

A crucial question to be addressed is how large time-bandwidth spreading of the radar signal energy we need to see the supremacy of the quantum radar compared to its classical counterpart. Is it possible to see a further improvement by spreading also in the space domain?

The use of a Quantum Radar as a low-probability-of-intercept (LPI) radar seems to be revealed as a key field of application, and is to be addressed. Likewise the supremacy in use in a heavily electromagnetically contested environment.

Uses of a Quantum Radar being more futuristic have been suggested. One is, that Quantum Illumination target detection could be used to unveil a cloaked target[16] [53].

[16] An electromagnetically cloaked target has been given such material properties that an electromagnetic field incident on the target is bent around it.

References

[1] "Demonstrating Quantum Supremacy," ed: YouTube.

[2] "WACQT | Wallenberg Centre for Quantum Technology." Chalmers. https://www.chalmers.se/en/centres/wacqt/Pages/default.aspx (accessed 2020-06-15).

[3] "Quantum Technologies Flagship." The European Commission. https://ec.europa.eu/digital-single-market/en/quantum-technologies (accessed 2020-06-15).

[4] M. J. Brandsema, "Formulation and Analysis of the Quantum Radar Cross Section," Ph. D. thesis, The Graduate School College of Engineering, The Pennsylvania State University, 2017.

[5] M. Lanzagorta, *Quantum Radar*. Morgan \& Claypool Publishers, 2011, p. 140.

[6] M. J. Brandsema, M. Lanzagorta, and R. M. Narayanan, "Quantum Electromagnetic Scattering and the Sidelobe Advantage," in *2020 IEEE International Radar Conference (RADAR)*, 28-30 April 2020 2020, pp. 755-760, doi: 10.1109/RADAR42522.2020.9114591.

[7] M. Höijer, T. Hult, and P. Jonsson, "Quantum Radar - A survey of the science, technology and litterature," Swedish Defence Research Agency FOI, Linköping, FOI-R--4854--SE, 2019. [Online]. Available: https://www.foi.se/en/foi/reports/report-summary.html?reportNo=FOI-R--4854--SE

[8] J. H. Shapiro, "Quantum illumination: From enhanced target detection to Gbps quantum key distribution," in *2017 Conference on Lasers and Electro-Optics (CLEO)*, San Jose, CA, USA, 14-19 May 2017 2017: IEEE, p. FTu3F.1. [Online]. Available: https://ieeexplore.ieee.org/stamp/stamp.jsp?tp=&arnumber=8083312&isnumber=8082845. [Online]. Available: https://ieeexplore.ieee.org/stamp/stamp.jsp?tp=&arnumber=8083312&isnumber=8082845

[9] J. H. Shapiro, "The Quantum Illumination Story : (Invited Paper)," in *2019 IEEE International Conference on Microwaves, Antennas, Communications and Electronic Systems (COMCAS)*, 4-6 Nov. 2019 2019, pp. 1-4, doi: 10.1109/COMCAS44984.2019.8958368.

[10] J. H. Shapiro, "The Quantum Illumination Story," *IEEE Aerospace and Electronic Systems Magazine,* vol. 35, no. 4, pp. 8-20, 2020, doi: 10.1109/MAES.2019.2957870.

[11] D. Luong, C. W. S. Chang, A. M. Vadiraj, A. Damini, C. M. Wilson, and B. Balaji, "Receiver Operating Characteristics for a Prototype Quantum Two-Mode Squeezing Radar," *IEEE Transactions on Aerospace and Electronic Systems,* vol. 56, no. 3, pp. 2041-2060, 2020, doi: 10.1109/TAES.2019.2951213.

[12] S. Barzanjeh, S. Pirandola, D. Vitali, and J. M. Fink, "Microwave quantum illumination using a digital receiver," *Science Advances,* vol. 6, no. 19, p. eabb0451, 08 May 2020, doi: 10.1126/sciadv.abb0451.

[13] J. H. Shapiro, "Defeating passive eavesdropping with quantum illumination," *Physical Review A,* vol. 80, no. 2, p. 022320, 08/17/ 2009, doi: 10.1103/PhysRevA.80.022320.

[14] J. H. Shapiro, Z. Zhang, and F. N. C. Wong, "Secure communication via quantum illumination," *Quantum Information Processing,* vol. 13, no. 10, pp. 2171-2193, 2014/10/01 2014, doi: 10.1007/s11128-013-0662-1.

[15] Q. Zhuang, Z. Zhang, J. Dove, F. N. C. Wong, and J. H. Shapiro, "Floodlight quantum key distribution: A practical route to gigabit-per-second secret-key rates," *Physical Review A,* vol. 94, no. 1, p. 012322, 07/14/ 2016, doi: 10.1103/PhysRevA.94.012322.

[16] Z. Zhang, Q. Zhuang, F. N. C. Wong, and J. H. Shapiro, "Floodlight quantum key distribution: Demonstrating a framework for high-rate secure communication," *Physical Review A,* vol. 95, no. 1, p. 012332, 01/26/ 2017, doi: 10.1103/PhysRevA.95.012332.

[17] Z. Zhang, C. Chen, Q. Zhuang, F. N. C. Wong, and J. H. Shapiro, "Experimental quantum key distribution at 1.3 gigabit-per-second secret-key rate over a 10 dB loss channel," *Quantum Science and Technology,* vol. 3, no. 2, p. 025007, 2018/04 2018, doi: 10.1088/2058-9565/aab623.

[18] J. H. Shapiro, D. M. Boroson, P. B. Dixon, M. E. Grein, and S. A. Hamilton, "Quantum low probability of intercept," *J. Opt. Soc. Am. B,* vol. 36, no. 3, pp. B41-B50, 2019/03/01 2019, doi: 10.1364/JOSAB.36.000B41.

[19] S. Lloyd, "Enhanced Sensitivity of Photodetection via Quantum Illumination," *Science,* vol. 321, no. 5895, p. 1463, 2008, doi: 10.1126/science.1160627.

[20] J. H. Shapiro and S. Lloyd, "Quantum illumination versus coherent-state target detection," *New Journal of Physics,* vol. 11, no. 6, p. 063045, 2009/06/24 2009, doi: 10.1088/1367-2630/11/6/063045.

[21] S.-H. Tan *et al.*, "Quantum Illumination with Gaussian States," *Physical Review Letters,* vol. 101, no. 25, p. 253601, 12/18/ 2008, doi: 10.1103/PhysRevLett.101.253601.

[22] S. Guha and B. I. Erkmen, "Gaussian-state quantum-illumination receivers for target detection," *Physical Review A,* vol. 80, no. 5, p. 052310, 11/10/ 2009, doi: 10.1103/PhysRevA.80.052310.

[23] Z. Zhang, S. Mouradian, F. N. C. Wong, and J. H. Shapiro, "Entanglement-Enhanced Sensing in a Lossy and Noisy Environment," *Physical Review Letters,* vol. 114, no. 11, p. 110506, 03/20/ 2015, doi: 10.1103/PhysRevLett.114.110506.

[24] D. Bacon, I. L. Chuang, and A. W. Harrow, "Efficient Quantum Circuits for Schur and Clebsch-Gordan Transforms," *Physical Review Letters,* vol. 97, no. 17, p. 170502, 10/27/ 2006, doi: 10.1103/PhysRevLett.97.170502.

[25] Q. Zhuang, Z. Zhang, and J. H. Shapiro, "Optimum Mixed-State Discrimination for Noisy Entanglement-Enhanced Sensing," *Physical Review Letters,* vol. 118, no. 4, p. 040801, 01/27/ 2017, doi: 10.1103/PhysRevLett.118.040801.

[26] S. Barzanjeh, S. Guha, C. Weedbrook, D. Vitali, J. H. Shapiro, and S. Pirandola, "Microwave Quantum Illumination," *Physical Review Letters,* vol. 114, no. 8, p. 080503, 02/27/ 2015, doi: 10.1103/PhysRevLett.114.080503.

[27] M. Lanzagorta, J. Uhlmann, O. Jitrik, S. E. Venegas-Andraca, and S. Wiesman, "Quantum computation of the Electromagnetic Cross Section of Dielectric targets," *SPIE Defence + Security,* vol. The International Society of optics and photonics, 2016.

[28] M. Lanzagorta and S. E. Venegas-Andraca, "Algorithmic analysis of Quantum Radar Sections," *SPIE Defence + Security,* vol. The International Society of optics and photonics, 2016.

[29] K. Liu, H. Xiao, H. Fan, and Q. Fu, "Analysis of Quantum Radar Cross Section and its Influence on Target Detection Performance," *IEEE Photonics Technology Letters,* vol. 26, no. 11, 2014.

[30] M. J. Brandsema, M. Lanzagorta, and R. M. Narayanan, "Equivalence of Classical and Quantum Electromagnetic Scattering in the Far-Field Regime," *IEEE Aerospace and Electronic Systems Magazine,* vol. 35, no. 4, pp. 58-73, 2020.

[31] F. Daum, "A system engineering perspective on quantum radar," in *2020 IEEE International Radar Conference (RADAR)*, Washington DC cahnged to online due to Covid-19, April 28 - 30, 2020, pp. 958-963.

[32] P. Massoud Salehi and J. Proakis, *Digital Communications*. McGraw-Hill Education, 2007.

[33] K. M. R. Audenaert *et al.*, "Discriminating States: The Quantum Chernoff Bound," *Physical Review Letters,* vol. 98, no. 16, p. 160501, 04/17/ 2007, doi: 10.1103/PhysRevLett.98.160501.

[34] D. Luong, S. Rajan, and B. Balaji, "Entanglement-Based Quantum Radar: From Myth to Reality," *IEEE Aerospace and Electronic Systems Magazine,* vol. 35, no. 4, pp. 22-35, 2020, doi: 10.1109/MAES.2020.2970261.

[35] S. L. Braunstein and P. van Loock, "Quantum information with continuous variables," *Reviews of Modern Physics,* vol. 77, no. 2, pp. 513-577, 06/29/ 2005, doi: 10.1103/RevModPhys.77.513.

[36] M. A. Nielsen and I. L. Chuang, *Quantum Computation and Quantum Information: 10th Anniversary Edition*. Cambridge University Press, 2010.

[37] C. Weedbrook *et al.*, "Gaussian quantum information," *Reviews of Modern Physics,* vol. 84, no. 2, pp. 621-669, 05/01/ 2012, doi: 10.1103/RevModPhys.84.621.

[38] U. L. Andersen, G. Leuchs, and C. Silberhorn, "Continuous-variable quantum information processing," *Laser & Photonics Reviews,* vol. 4, no. 3, pp. 337-354, 2010/04/28 2010, doi: 10.1002/lpor.200910010.

[39] U. Andersen, J. Neergaard-Nielsen, P. Loock, and A. Furusawa, "Hybrid discrete- and continuous-variable quantum information," *Nature Physics,* vol. 11, pp. 713-719, 09/01 2015, doi: 10.1038/nphys3410.

[40] J. W. Gibbs, *Elementary Principles in Statistical Mechanics*. New York: Charles Scribner's Sons, 1902.

[41] L. Boltzmann, K. Sharp, and F. Matschinsky, "Translation of Ludwig Boltzmann's Paper: On the Relationship between the Second Fundamental Theorem of the Mechanical Theory of Heat and Probability Calculations Regarding the Conditions for Thermal Equilibrium," *Mathematisch-Naturwissen Classe. Abt. II, LXXVI 1877,* pp. 373-435.

[42] J. B. Johnson, "Thermal Agitation of Electricity in Conductors," *Physical Review,* vol. 32, no. 110, pp. 97-109, 1928.

[43] H. Nyquist, "Thermal Agitation of Electric Charge in Conductors," *Physical Review,* vol. 32, no. 110, pp. 110-113, 1928.

[44] J. D. Breeze, E. Salvadori, J. Sathian, N. M. Alford, and C. W. M. Kay, "Continuous-wave room-temperature diamond maser," *Nature,* vol. 555, no. 7697, pp. 493-496, 2018/03/01 2018, doi: 10.1038/nature25970.

[45] H. Heffner, "The Fundamental Noise Limit of Linear Amplifiers," *Proceedings of the IRE,* vol. 50, no. 7, pp. 1604-1608, 1962, doi: 10.1109/JRPROC.1962.288130.

[46] C. M. Caves, "Quantum limits on noise in linear amplifiers," *Physical Review D,* vol. 26, no. 8, pp. 1817-1839, 1982.

[47] J. Bourassa and C. M. Wilson, "Amplification Requirements For Quantum Radar Signals," in *2020 IEEE International Radar Conference (RADAR)*, Washington, DC, USA, 28-30 April 2020: IEEE, pp. 973-978, doi: 10.1109/RADAR42522.2020.9114574.

[48] D. Braun *et al.*, "Quantum-enhanced measurements without entanglement," *Reviews of Modern Physics,* vol. 90, 2018.

[49] C. W. S. Chang, A. M. Vadiraj, J. Bourassa, B. Balaji, and C. M. Wilson, "Quantum-enhanced noise radar," *Applied Physics Letters,* vol. 114, no. 11, 2019.

[50] T. C. White *et al.*, "Traveling wave parametric amplifier with Josephson junctions," *Applied Physics Letters,* vol. 106, 2015.

[51] G. S. Agarwal and S. Chaturvedi, "How much quantum noise is detrimental to entanglement," *Elsevier Optics Communications,* vol. 283, no. 5, pp. 839-842, 2009.

[52] R. G. Torromé, N. B. Bekhti-Winkel, and P. Knott, "Introduction to quantum radar," *arXiv preprint arXiv:2006.14238,* 2020. [Online]. Available: https://arxiv.org/abs/2002.12252.

[53] U. Las Heras, R. Di Candia, K. G. Fedorov, F. Deppe, M. Sanz, and E. Solano, "Quantum illumination reveals phase-shift inducing cloaking," *Scientific Reports,* vol. 7, no. 1, p. 9333, 2017/08/24 2017, doi: 10.1038/s41598-017-08505-w.

[54] R. J. Glauber, "Photon Correlations," *Physical Review Letters,* vol. 10, no. 3, pp. 84-86, 02/01/ 1963, doi: 10.1103/PhysRevLett.10.84.

[55] G. Björk and J. Söderholm. "The Dirac notation in quantum optics." https://www.kth.se/social/files/54b2a1fdf2765442623b878b/Dirac_notation_pm_r4.pdf (accessed 2020-09-25).

Appendix – Coherent states and common detection methods

The coherent state

The coherent state was introduced by Glauber[17] [54] and is the quantum mechanical description of the state that most resembles a classical description of a coherent electromagnetic field with phase and intensity. The Heisenberg uncertainty principle is embedded in the state and the shot noise is explained by the state itself rather than in the detection process as in the semiclassical description. A state that could be described as a coherent state, or mixture of several coherent states, is often called a *classical* state in quantum mechanics. Such states can be treated with the semiclassical theory and give the same results as the quantum description, and therefore, the term coherent states is sometimes used as equivalent to classical states. However, if the state breaks any of the restrictions of a classical field description, e.g. number states (fixed number of photons) or the squeezed state (see section 4.4), the semiclassical theory will not give the correct result. The strength with quantum mechanical description of the coherent state is that theory previously explained in the semiclassical picture can be treated in quantum theory in a straightforward way. It also gives a good picture of the implication the Heisenberg uncertainty principle. To show some characteristics of the coherent state we use Dirac notation. A good introduction for those not familiar with the notation is given in a PM from KTH [55].

The coherent state is denoted by $|\alpha\rangle$, where α is a complex number, and the coherent state is defined by,

$$\hat{a}|\alpha\rangle = \alpha|\alpha\rangle,$$

where $\hat{a}$ is the annihilation operator. The number-state expansion of the coherent state is

$$|\alpha\rangle = \exp\left(\frac{|\alpha|^2}{2}\right)\sum_n \frac{\alpha^n}{\sqrt{n!}}|n\rangle \ .$$

Note, the coherent state has an indefinite number of photons and a Poison distribution,

$$P(n) = |\langle n|\alpha\rangle|^2 = \frac{|\alpha|^{2n}}{n!}\exp(-|\alpha|^2) \ .$$

The expectation value and the variance, respectively, of the photon number is

$$\langle\hat{n}\rangle = \langle(\Delta\hat{n})^2\rangle = |\alpha|^2.$$

Hence, the shot noise is a result of the Poison distribution of the photon numbers in the coherent state.

If we instead are interested in the phase of the coherent state, we use the quadrature operators

$$\hat{a}_1 \equiv \frac{1}{2}\left(\hat{a} + \hat{a}^\dagger\right) \text{ and } \hat{a}_2 \equiv \frac{1}{2i}\left(\hat{a} - \hat{a}^\dagger\right),$$

[17] Glauber was awarded the Nobel Prize in Physics in 2005 for his development of the coherent state.

where $\hat{a}$ and $\hat{a}^{\dagger}$ are the annihilation and creator operators, respectively. The quadrature operators do not commute, which results in a Heisenberg's uncertainty when measuring both quadratures of a state. The expectation values for the quadrature operators on a coherent state $|\alpha\rangle$ are

$$\langle \hat{a}_1 \rangle = \mathrm{Re}\{\alpha\} \text{ and } \langle \hat{a}_2 \rangle = \mathrm{Im}\{\alpha\}$$

and the variances are

$$\langle \Delta \hat{a}_1{}^2 \rangle = \langle \Delta \hat{a}_2{}^2 \rangle = \frac{1}{4}.$$

In quantum mechanics several notations of the quadrature, such as X_1 and X_2; Q and P, are used, but here we use I and Q, in-phase and the quadrature components, respectively.

Figure 9 shows examples of samples of two coherent states. The blue dots show $|\alpha = 0\rangle$, the vacuum state, which is the same as the Heisenberg minimum uncertainty vacuum state. The red dots show $|\alpha = 10/\sqrt{2} + i\,10/\sqrt{2}\rangle$, where $|\alpha|^2 = 100$, i.e. the expectation value and the variance of the photon number is 100. The graph can be seen as frozen in time and space. If we measure a moment later the red dots have rotated along the circle and after one period $T = 1/f$, where f is the frequency of the electromagnetic field, the dots are back on the same position.

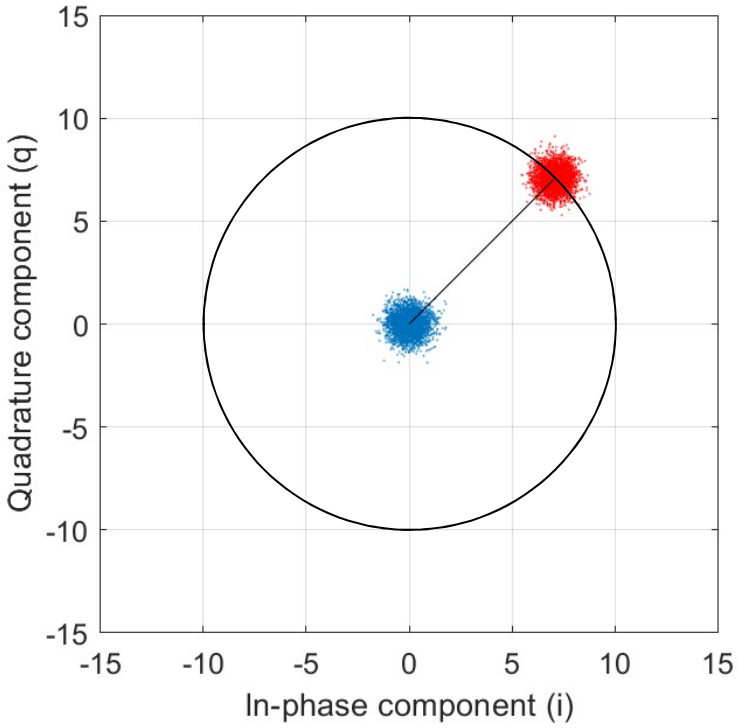

Figure 9. In the figure 4000 samples of two different coherent states are shown. The blue samples show $\alpha = 0$, which is the same as the Heisenberg minimum uncertainty vacuum state. The red samples show $\alpha = 10/\sqrt{2} + i\,10/\sqrt{2}$, where the amplitude of α is 10.

Common detection methods

The most common receivers are shown in Figure 10. These are closely related to the operators described in the previous section, the number-state operator and the quadrature operators.

Direct detection is a photon number measurement letting the number state operator operate on the signal. In practice, it is an energy detector measuring directly on the signal s. No phase information is obtained in the measurement.

In the homodyne and heterodyne detection, one or two quadratures of the state are measured. This is done by mixing the signal with a strong local oscillator (LO). In homodyne the LO has the same frequency as the signal whereas in heterodyne the LO has a different frequency than the signal. After the mixing, the combined state are normally measured with an energy detector and the quadrature can be determined in respect to the phase of the LO. It can be shown that in a balanced homodyne measurement (50/50 mixing), one quadrature in signal s can be measured without introducing extra noise by subtracting the measurement in d_1 with the measurement in d_2.

Normally, both quadratures are measured by use of heterodyne detection. It can also be measured in a double homodyne detector by dividing the signal s in two parts and performing homodyne detection on each part where the two LOs are phase shifted by ninety degrees. Measuring both quadratures of the same signal will always introduce an extra 3 dB noise regardless which method is used, heterodyne or a double homodyne detection. The reason is that the quadrature operators do not commute. Hence, they cannot be perfectly measured due to the Heisenberg's uncertainty principle.

Sometimes in the quantum literature, heterodyne detection is equated with measuring both quadratures rather than measuring with different signal and LO frequencies. This can cause some confusion.

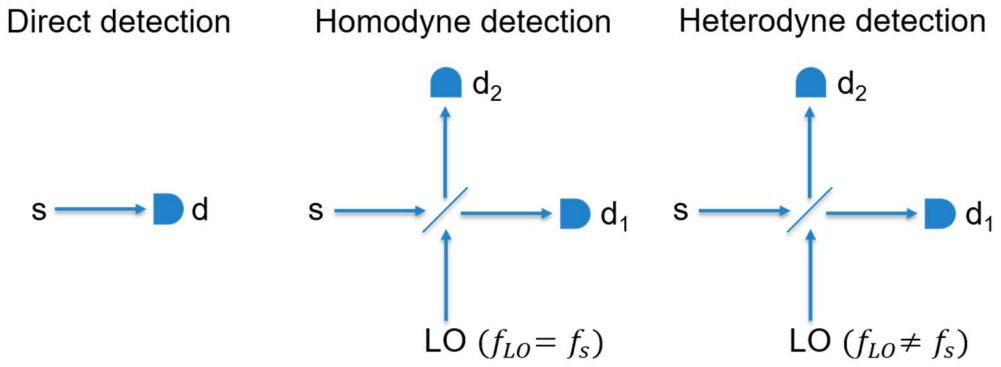

Figure 10. Common detection methods, direct, homodyne and heterodyne detection, where s is the signal or state that is measured, $d_{(x)}$ are detectors, LO is a local oscillator, f_s and f_{LO} are the frequency of the signal and local oscillator respectively.

FOI, Swedish Defence Research Agency, is a mainly assignment-funded agency under the Ministry of Defence. The core activities are research, method and technology development, as well as studies conducted in the interests of Swedish defence and the safety and security of society. The organisation employs approximately 1000 personnel of whom about 800 are scientists. This makes FOI Sweden's largest research institute. FOI gives its customers access to leading-edge expertise in a large number of fields such as security policy studies, defence and security related analyses, the assessment of various types of threat, systems for control and management of crises, protection against and management of hazardous substances, IT security and the potential offered by new sensors.

FOI
Defence Research Agency
SE-164 90 Stockholm

Phone: +46 8 555 030 00
Fax: +46 8 555 031 00

www.foi.se